Laser and Particle Beams (1989), *vol.* 7, *part* 3, *pp.* 627–635
Printed in Northern Ireland

Non-uniform target illumination in deflagration regime. Refractive smoothing

By J. A. NICOLÁS, J. SANZ, J. R. SANMARTÍN, AND J. HILARIO
Escuela Técnica Superior de Ingenieros Aeronáuticos, Universidad Politécnica, 28040-Madrid, Spain

(Received 28 November, 1988)

Refractive smoothing of weak non-uniformities in the illumination of laser targets is analyzed, assuming absorption at the critical density and restricting conduction to a thin layer, and using results from thermal smoothing, which is uncoupled from the refraction. Magnetic effects are included. Non-uniformity wavelengths comparable to the thickness of the conduction layer are considered; efficient smoothing exists at both short and long wavelengths in this range. Thermal focusing could make the ablated plasma unstable.

1. Introduction

One main obstacle facing the direct-drive approach to laser fusion is its sensitiveness to non-uniformities in the driving. Thermal conduction was considered in the past as a possible mechanism for the smoothing of irradiation non-uniformities (Gardner & Bodner 1981). Such a smoothing mechanism operates in the overdense part of the escaping corona: Heat conduction takes the energy absorbed at or below the critical density n_c, to the ablation surface, where target compression and acceleration occurs. However, other mechanisms such as refraction and inverse Bremsstrahlung could affect the fate of non-uniformities in the underdense corona. Here we consider refraction effects (Sanmartín *et al.* 1987). Other interrelated smoothing processes are the random phase (Kato *et al.* 1984), ISI (Obenschain *et al.* 1986), the fly eye (Deng & Yu 1984) and broad band lasers (Lin *et al.* 1986). We have recently (Sanz *et al.* 1988) analyzed thermal smoothing in some simple limit regime: (i) irradiation almost uniform and at normal incidence: (ii) deflagration conditions, i.e., conduction restricted to a thin layer next to the target; and (iii) absorption only at the critical surface. It then follows that the layer had both overdense and underdense parts, while the large region outside was isentropic and entirely underdense. Also, it was possible to uncouple the joint study of thermal and refractive smoothing: this allowed us to entirely determine the flow structure for a given irradiation perturbation reaching the critical surface, with no regard for the underdense refraction.

The purpose of the present work is to relate the patterns of irradiation at the entrance to the layer and at the critical surface to each other so that the previous results (Sanz *et al.* 1988) may then be stated in terms of the far-away irradiation reaching the corona. In the present deflagration regime an analysis of the conduction layer sufficed to determine thermal smoothing. Refraction, however, may take place both in the underdense part of the layer and in the underdense isentropic flow outside it. Here we avoid the study of the isentropic region by considering non-uniformity wavelengths comparable to the layer thickness; this point will be elaborated at the end.

In §§ 2 and 3 we briefly review the analysis of Sanmartin *et al.* 1987, and determine

0263-0364/89/0703–0627$05.00

subito e.V. licensed customer copy supplied and printed for Universidad Politecnica de Madrid. Servicio de Coordinacion de Bibliotecas (SLI04X00177E)

the refraction, respectively. In § 4 we discuss numerical results. Finally, conclusions are given in § 5. An important conclusion of our work is that under some conditions thermal self-focusing (Estabrook *et al.* 1985) may turn the coronal flow unstable.

2. Thermal smoothing

Since the conduction layer is thin, it can be analysed by means of quasisteady equations. Note that for given n_c, intensity I, and target or focal radius R, the isentropic flow outside will be also quasisteady (and divergent) for a pulse duration τ_L long enough; the flow will be unsteady and planar in the opposite limit. A deflagration regime will exist for large τ_L, I^{-1}, n_c, and R.

In the analysis of thermal smoothing the equations of ion continuity, electron momentum and energy, and total momentum, were used together with Ampere and Faraday's laws. The ion temperature could be ignored because of a large ion charge number. Braginskii's results (1965) for both electron heat flux and ion-electron friction were also used. Since the non-uniformity was weak, it was sufficient to consider Righi–Leduc and Nernst terms in addition to the usual Fourier (Spitzer) and Ohm's laws; there are no thermoelectric effects.

Light impinged, from the right, on a *highly overdense* target. The receding of its (ablation) surface had then a negligible effect on the behavior of the entire expanding corona, and, in particular, of its conduction layer. Thus the ablation surface was simply set at $x = 0$, where the density was let to go to infinity.

For uniform irradiation I_{c0} at n_c, the laser heating term is $I_{c0}\delta(x - x_{c0})$. The analysis of that case yields fluid profiles, $n_0(x)$, velocity $v_0(x)$ and temperature $T_0(x)$, and such quantities as ablation pressure P_{a0}, mass ablation rate $\dot{m}_{a0}$, and the location x_{c0} where $n_0 = n_c$. Sanz *et al.* (1988) considered then a weakly non-uniform irradiation at the critical surface

$$I_c = I_{c0} + I_{c1} \exp(i k y), \quad I_{c1}/I_{c0} \ll 1,$$

the surface location being

$$x_c = x_{c0} + x_{c1} \exp(i k y) + \ldots$$

with x_{c1}/x_{c0} small and unknown. To avoid mathematical difficulties at x_{c0}, the x coordinate was strained in the form (Van Dyke 1964)

$$x = s\left(1 + \frac{x_{c1}}{x_{c0}} \exp(i k y) + \ldots\right) \tag{1}$$

s, y being new variables. In this way we had $s = x_{c0}$ at $x = x_c$, to all orders in I_{c1}/I_{c0}. Expanding variables $n = n_0(s) + n_1(s) \exp(i k y) + \ldots$, first order linearized equations were obtained; they are rewritten in the Appendix. First order profiles such as $n_1(s)$, $T_1(s), \ldots$, and particular values of interest (x_{c1}, $P_{a1}, \ldots$) were determined. These last results depend on kx_{c0} and on a second dimensionless parameter Λ_c, which is also given in the Appendix. The influence of Λ_c was found to be weak.

3. Underdense refraction

The first-order transverse variation of density refracts the light propagating inwards. Clearly the refraction has no local effect on the flow and does not modify the relation between I_{c1}, x_{c1}, and $n_1(s)$.

Let ε be the dielectric function $(1 - n/n_c)$ of a non-relativistic plasma, $\bar{\tau}$ the unit

subito e.V. licensed customer copy supplied and printed for Universidad Politecnica de Madrid. Servicio de Coordinacion de Bibliotecas (SLI04X00177E)

vector along an incoming ray, and I the local light intensity. The propagation equations are (Landau & Liftshitz 1980)

$$\bar{\tau}\,.\,\nabla\bar{\tau} = \frac{1}{2\varepsilon}[\nabla\varepsilon - \bar{\tau}(\bar{\tau}\,.\,\nabla\varepsilon)] \tag{2}$$

for the ray trajectory, and

$$\nabla\,.\,(\bar{\tau}\,I) = 0, \tag{3}$$

for the conservation of light energy. We then expand the new quantities, using the variables introduced in § 2:

$$I = I_0 + I_1(s)\exp(i\,k\,y) + \ldots, \quad (I_0 \equiv I_{c0})$$
$$\tau_y \equiv \tau_{y1}(s)\exp(i\,k\,y) + \ldots,$$
$$\varepsilon = 1 - n_c^{-1}[n_0(s) + n_1(s)\exp(i\,k\,y) + \ldots],$$

and $\tau_x = -1 +$ 2nd-order terms. Linearizing equations (2), (3) we get

$$\frac{dI_1}{ds} = I_0 k(i\tau_{y1})$$
$$2\left(1 - \frac{n_0}{n_c}\right)\frac{d}{ds}(i\tau_{y1}) = (i\tau_{y1})\frac{d}{ds}\frac{n_0}{n_c} - k\left(\frac{n_1}{n_c} - s\frac{x_{c1}}{x_{c0}}\frac{d}{ds}\frac{n_0}{n_c}\right) \tag{4}$$

As it is well known, and because $d\varepsilon/dn$ is negative, a plasma refracts light into lower-density regions. The first term on the right-hand side of (4) is due to the longitudinal density gradient; if alone, it would yield $\tau_{y1} \propto (1 - n_0/n_c)^{-\frac{1}{2}}$: an oblique ray approaching the critical surface would turn further (the singularity at n_c presents no difficulties). The other terms arise from the transverse density gradient, the last one coming from $n_0(s) \simeq n_0(x) + (s - x)dn_0/dx$, with $(s - x)$ given in equation (1).

The boundary conditions are

$$I_1 = I_{c1} \quad \text{at} \quad s = x_{c0},$$
$$\tau_{y1} \to 0 \quad \text{as} \quad s/x_{c0} \to +\infty, \text{ (normal incidence).}$$

One then obtains

$$I_{\infty 1} = I_{c1}\left(1 + \int_{x_{c0}}^{\infty} \frac{i\tau_{y1}}{I_{c1}/I_{c0}}\,k\,ds\right), \tag{5}$$

$$2i\tau_{y1} = k(1 - n_0/n_c)^{-\frac{1}{2}}\int_s^{\infty}[1 - n_0(s')/n_c]^{-\frac{1}{2}}\left(\frac{n_1(s')}{n_c} - s'\frac{x_{c1}}{x_{c0}}\frac{d}{ds'}\frac{n_0(s')}{n_c}\right)ds'. \tag{6}$$

It is convenient to define

$$\alpha \equiv -\int_{x_{c0}}^{\infty} \frac{i\tau_{y1}}{I_{c1}/I_{c0}}\,k\,ds,$$

so that

$$I_{c1} = I_{\infty 1} + \alpha I_{c1} \tag{7}$$

The dimensionless quantity α, which reflects the structure of the perturbed flow, depends on both kx_{c0} and Λ_c.

The perturbed density $n_1(s)$ is the sum of two parts: (i) a term $(x_{c1}/x_{c0})s\,dn_0/ds$, satisfying the non-homogeneous system (A.1–A.5) of differential equations, and (ii) fundamental solutions or modes of that system in homogeneous form (setting x_{c1}, $I_{c1} = 0$). One mode diverges as $s/x_{c0} \to +\infty$ and was excluded from the solution. We note here, for later reference, the behaviour of the other four modes at large s/x_{c0}. For

subito e.V. licensed customer copy supplied and printed for Universidad Politecnica de Madrid. Servicio de Coordinacion de Bibliotecas (SLI04X00177E)

low kx_{c0} we find

$$n_1 \sim \exp\left[-0{\cdot}435(1 \pm 3^{\frac{1}{2}}i)(k^2/x_{c0})^{\frac{1}{3}}s\right], \tag{8}$$

$$n_1 \sim \exp\left(-2{\cdot}28k^2x_{c0}s\right), \tag{9}$$

and for high kx_{c0},

$$n_1 \sim \exp\left[\pm i\left(\frac{2}{3}\right)^{\frac{1}{2}}k - \frac{0{\cdot}841}{x_{c0}}\right]s, \tag{10}$$

$$n_1 \sim \exp\left(-ks\right), \tag{11}$$

and similarly for T_1. The last mode is such that $n_1 \sim s^{-3}$ in either case.

4. Discussion of results

Figure 1 shows $I_{c1}/I_{\infty 1}$ versus kx_{c0} for limiting values of Λ_c. There is no sensible dependence on this parameter. Particularly, results that neglect altogether current and magnetic effects are valid in practice for $\Lambda_c = 0$.

The dependence on kx_{c0} presents, however, some interesting features. Let y_+ be the y range for which excess light intensity reaches, and is absorbed at the critical surface (a y_- range having a deficit intensity at n_c). Without loss of generality we set $I_{c0} > 0$ in equation (7)

$$\frac{I_{c1}}{I_{\infty 1}} = \frac{1}{1-\alpha}.$$

Notice that $\alpha(\Lambda_c, kx_{c0})$ is independent of I_{c1}. If $\alpha < 0$, we have $I_{\infty 1} > I_{c1} > 0$: light is refracted from y_+ into y_-, so that the underdense transverse density gradient must

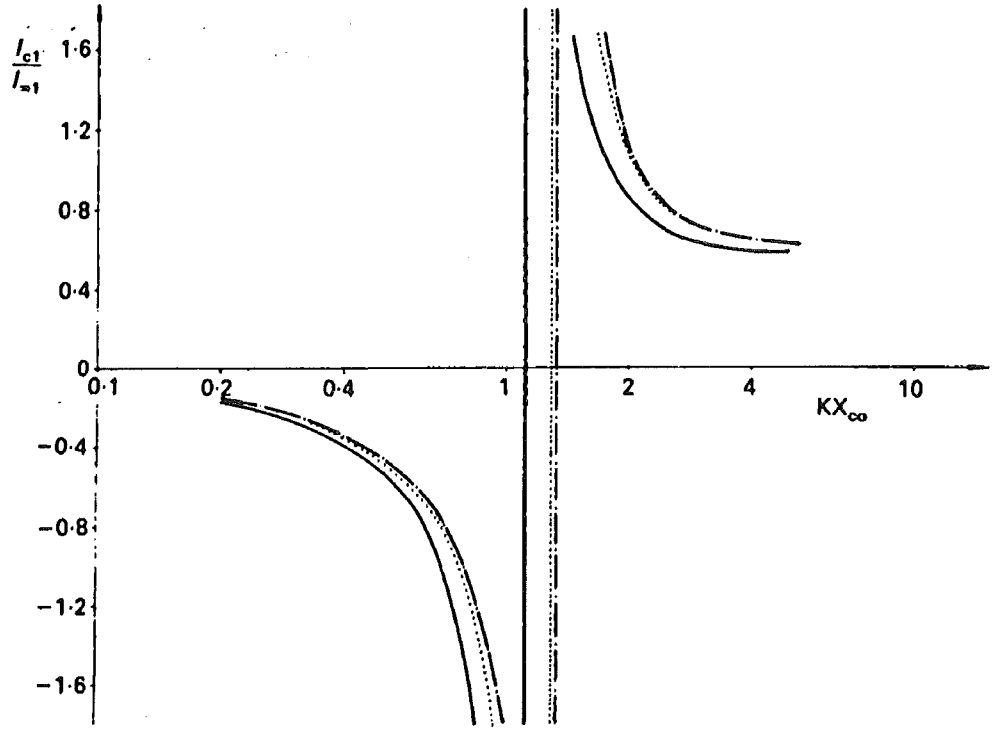

FIGURE 1. Critical-to-incident perturbed intensity ratio versus perturbation wavenumber k for a large (——) or small (· · ·) ratio of electron mean free path at critical density to laser wavelength; x_{c0} is the distance between critical and ablation surfaces. Results obtained neglecting entirely magnetic effects are also shown (– · –).

subito e.V. licensed customer copy supplied and printed for Universidad Politecnica de Madrid. Servicio de Coordinacion de Bibliotecas (SLI04X00177E)

point, on the average, the other way. Opposite conditions occur for positive α. In fact, if $\alpha > 1$, then $I_{\infty 1}$ would be negative, so that more light would be refracted into a y_+ range than excess light reaches n_c there. Figure 1 shows that this is indeed the case for k less than a value k^* close to $1/x_{c0}$.

This effect arises from the inefficiency of lateral heat conduction at long wavelengths (low k). Figure 2 shows the rippled critical surface and the transverse gradients for low k. The surface is farther from the target and hotter in y_- (Sanz *et al.* (1988), showed that x_{c1} at low k, and T_{c1}, are positive for $I_{c1} > 0$). As one moves outwards from the critical surface the initial transverse pressure gradient results in lateral motion, and soon dies off. The far away plasma however remains hotter in y_+, so that the transverse density gradient is now inverted. Hence, the far underdense plasma must refract light into y_+. When the light-ray approaches the critical surface, the opposite density gradient competes with the longitudinal one, and may be unable to turn back the ray into y_- leading to $\alpha > 1$.

For k very small the temperature perturbation will extend a long distance in the underdense plasma, lateral heat conduction being very inefficient. This is verified in equation (9) for the slowest decaying mode in the perturbation, which requires a die-off length $s \sim 1/x_{c0}k^2$, growing fast with decreasing k, thus producing $\alpha \gg 1$. Actually, for $kx_{c0} \to 0$ the integral defining α diverges, $\alpha \sim (kx_{c0})^{-2}$. Consequently $I_{c1}/I_{\infty 1} \sim -(kx_{c0})^2$: a small excess intensity I_{c1} produces a weak but long standing density gradient, that smooths off the driving non-uniformity $I_{\infty 1}$ (see figure 1).

As k increases α goes down continuously, reaching unity at some value k^* (vertical asymptote in figure 1). At this wavenumber the refraction produced by any excess

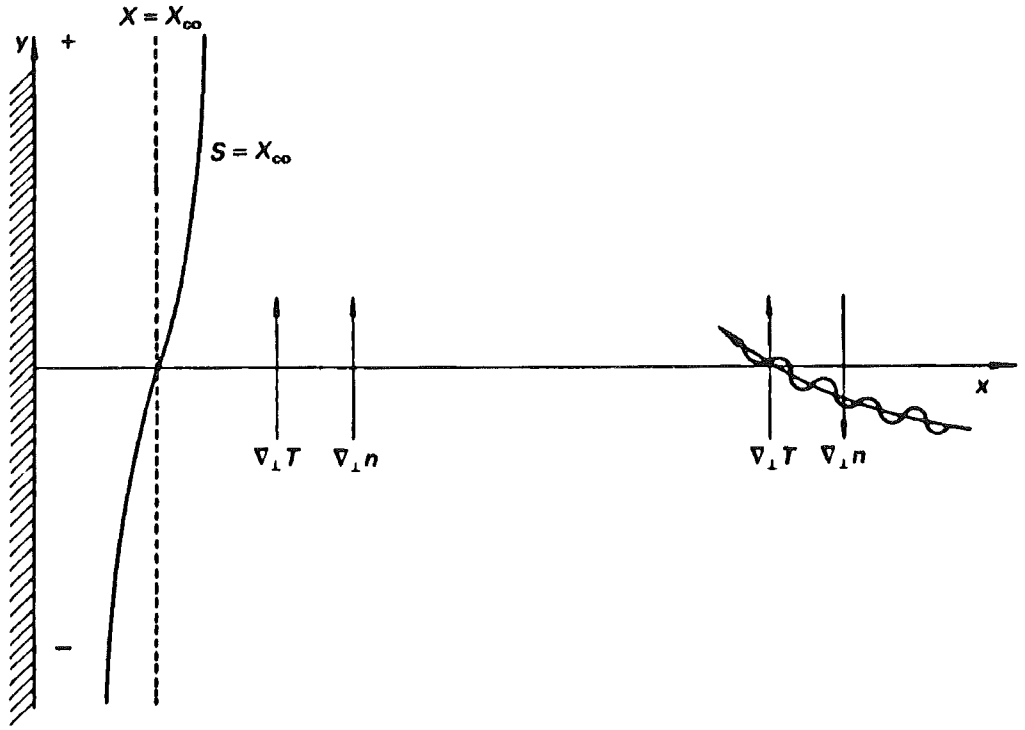

FIGURE 2. Schematics of conduction layer for wavenumber $k \ll 1/x_{c0}$, showing transverse gradients and perturbed (——) and unperturbed (– – –) critical surface. Transverse regions with excess or defect intensity at that surface are marked + or − ; x is along the main direction across the layer.

subito e.V. licensed customer copy supplied and printed for Universidad Politecnica de Madrid. Servicio de Coordinacion de Bibliotecas (SLI04X00177E)

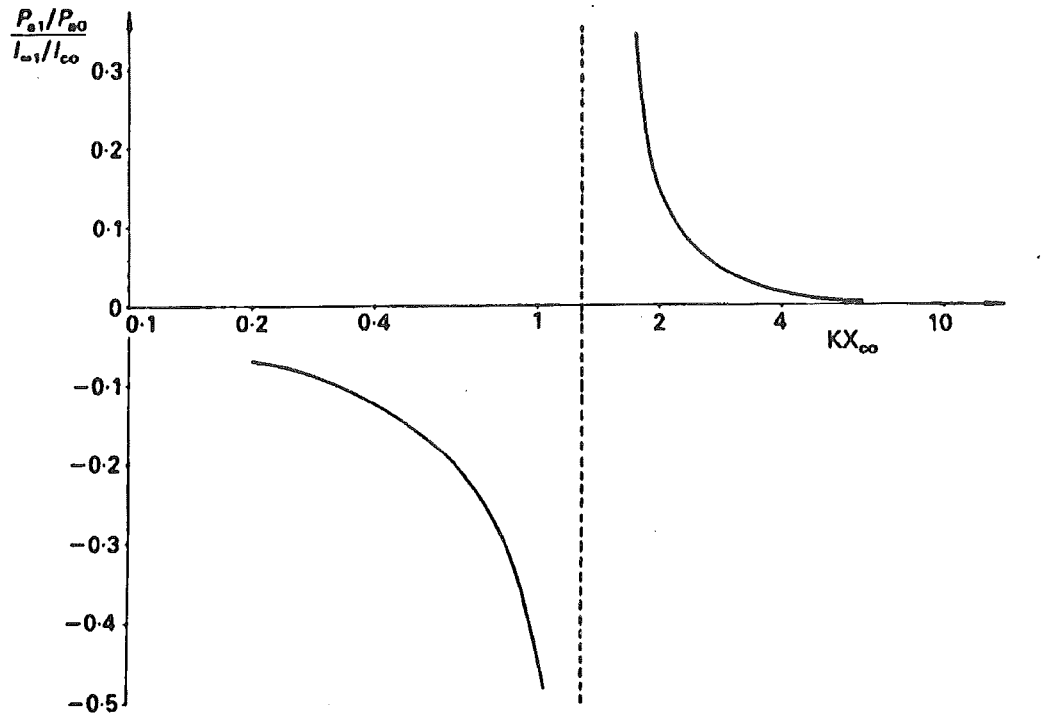

FIGURE 3. Perturbed ablation pressure normalized with perturbed incident intensity versus wavenumber; no magnetic effects included.

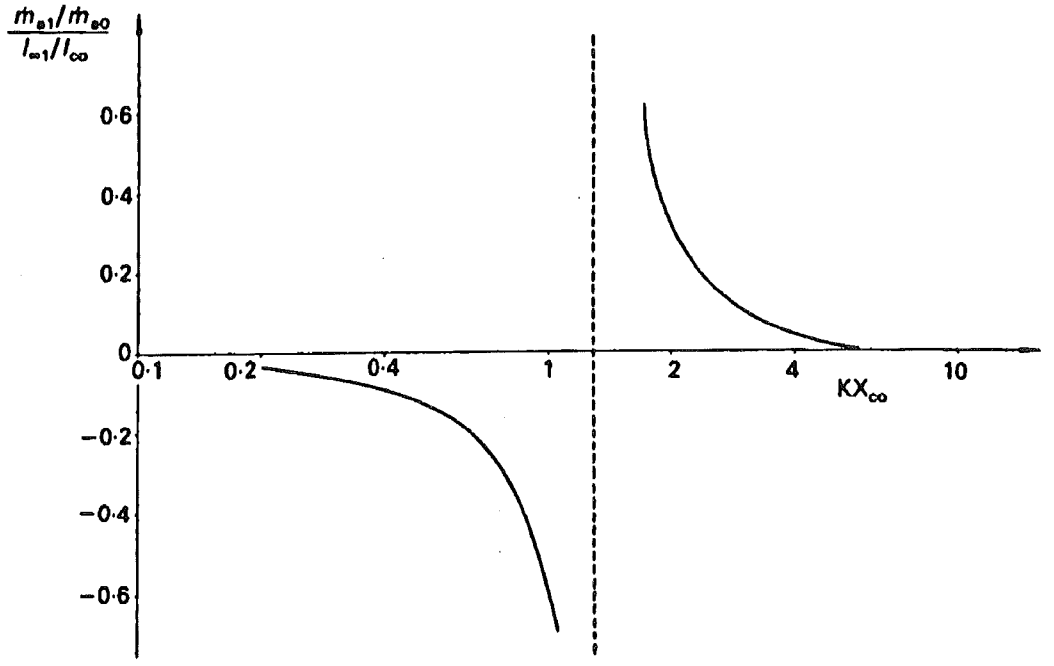

FIGURE 4. Perturbed mass ablation rate normalized with perturbed incident intensity versus wavenumber; no magnetic effects included.

subito e.V. licensed customer copy supplied and printed for Universidad Politecnica de Madrid. Servicio de Coordinacion de Bibliotecas (SLI04X00177E)

intensity I_{c1} would be just enough to get that excess at n_c. No driving $I_{\infty 1}$ would be required.

We now notice the following consequence of this fact. In a hypothetical stability analysis, one would set $I_{\infty 1} = 0$ from the start, retaining time derivatives in first-order quantities through a factor $e^{i\omega t}$, as usual. Then our present results show that one would get $\omega(k) = 0$ at $k = k^*$. This suggests that the wavenumber k^* could mark the separation between a stable range above k^*, and an unstable one below (though there might be other branches of the dispersion relation). At low k, indeed, the same arguments explaining why $I_{c1}/I_{\infty 1}$ is negative suggest that, for $I_{\infty 1} = 0$, any perturbation in the absorbed intensity I_c at n_c will produce density gradients that would feed back the intensity perturbation (Sanmartín *et al.* 1987). An analysis of this *overall* thermal focusing instability, is now in progress.

Figures 3 and 4 present perturbed ablation pressure P_{a1} and mass ablation rate $\dot{m}_{a1}$, normalized with $I_{\infty 1}$, obtained by using figures 2 and 4 in the work of Sanz *et al.* (1988), and figure 1 here. It proved difficult to reach $kx_{c0} \sim 10$ in figure 1 because of the rapid behavior of the mode given by (10); at such k, however, thermal smoothing of P_{a1}, $\dot{m}_{a1}$, etc., is very efficient.

5. Conclusions

We have analysed the refractive smoothing of non-uniformities in the irradiation reaching a laser target. We assumed (i) absorption at the critical density n_c, (ii) heat conduction restricted to a thin layer next to the target, i.e. layer thickness, or distance x_{c0} from critical to ablation surface, small compared with the overall length L of coronal plasma, (iii) weak non-uniformity, (iv) its wavenumber k of order $1/x_{c0}$.

Effective smoothing was found at both small and large kx_{c0}, that is, the critical-to-incident peak excess-intensity ratio, $I_{c1}/I_{\infty 1}$, was small. We explained the efficient smoothing at very low kx_{c0} by noting that lateral heat conduction is then much slower than pressure equalization: *opposite* transverse gradients for temperature and density persist a long distance along the main direction, across the layer:

$$\text{density perturbation decay length} \sim 1/x_{c0}k^2. \tag{12}$$

The ratio $I_{c1}/I_{\infty 1}$ was negative for k below some value close to $1/x_{c0}$ (more light is refracted into a transverse range for which excess intensity reaches n_c, than that excess itself). This is again explained by poor conduction at low k, and conditions near the critical surface: the far-downstream transverse temperature gradient points into ranges with excess intensity at n_c, the density gradient necessarily being opposite. We suggested that this thermal focusing could make the corona unstable. Thermomagnetic or Rayleigh–Taylor instabilities are not relevant to the phenomenon (magnetic effects were weak and target acceleration was neglected).

The validity of the analysis is limited by the use of assumptions (i) and (ii), which are somewhat contradictory (the first being reasonable at high intensity, the second at low). Work in progress at present is concerned with removing these limitations by including inverse bremsstrahlung absorption below n_c and effects of conduction throughout the corona. Electron transport where collisions are not frequent enough should be considered too. Assumption (iii) is reasonable since uniform target illumination is a condition strived for everywhere.

Our analysis obviously fails if density perturbations reach beyond the conduction layer, because then, refraction in the large coronal region outside must be taken into account. This occurs when the length (12) is comparable to L. For a spherical target

subito e.V. licensed customer copy supplied and printed for Universidad Politecnica de Madrid. Servicio de Coordinacion de Bibliotecas (SLI04X00177E)

and a long pulse, L is the target radius R and (12) gives

$$k \sim 1/(x_{c0}R)^{\frac{1}{2}}; \tag{13}$$

at these wavenumbers both spherical effects and conduction must be considered. As previously mentioned, at low kx_{c0} we have $-I_{c1}/I_{\infty 1} \sim (kx_{c0})^2$. Equation (13) then shows that our analysis is valid down to a minimum $I_{c1}/I_{\infty 1} \sim x_{c0}/R$. At still longer wavelengths, $k \sim 1/R$, recently analyzed by Pérez-Saborid, Barrero & Sanz, only refraction outside the layer is important. Wavenumbers $k \sim 1/R$ could arise from irradiation asymmetries due to a short number of incident beams; wavenumbers $k \sim 1/x_{c0}$ could correspond to short scale irregularities across the section of each single beam caused by the Induced Spatial Incoherence Technique.

Acknowledgement

This research was supported by the Comisión Asesora de Investigación Científica y Técnica (PB85 59 CO201) and the Instituto de Fusión Nuclear of Spain.

Appendix

Expanding variables to first order $n = n_0(s) + n_1(s)\exp(iky)$ and similarly for T, and longitudinal and transverse velocities v_x and v_y, and linearizing the equations of ion continuity, total momentum and electron energy, we obtained to first order a fifth-order system of ordinary differential equations with variable coefficients for n_1, v_{x1}, v_{y1} and T_1 (Sanz *et al.* 1988):

$$\frac{d}{ds}(v_0 n_1 + n_0 v_{x1}) + ikn_0 v_{y1} = 0, \tag{A.1}$$

$$\frac{d}{ds}\left(2\dot{m}_{a0}v_{x1} + P_{a0}\frac{n_1}{n_0} + n_0 T_1\right) + ik\dot{m}_{a0}v_{y1} = 0, \tag{A.2}$$

$$\dot{m}_{a0}\frac{dv_{y1}}{ds} + ik(n_0 T_1 + T_0 n_1) = -\dot{m}_{a0}ik\frac{x_{c1}}{x_{c0}}s\frac{dv_0}{ds}, \tag{A.3}$$

$$\begin{aligned}(n_0 v_{x1} + v_0 n_1)\frac{d}{ds}\left(\tfrac{1}{2}\bar{m}v_0^2 + \tfrac{5}{2}T_0\right) + \frac{d}{ds}v_0\left(\tfrac{5}{2}n_0 T_1 + \dot{m}_{a0}v_{x1}\right)\\ + \left(k^2 - \frac{d^2}{ds^2}\right)\bar{K}T_0^{\frac{1}{2}}T_1 + \frac{\bar{K}T_0^{\frac{1}{2}}\,dT_0/ds}{\gamma_0 n_0 v_0}\left(\tfrac{3}{2} - \frac{T_0\,dn_0/ds}{n_0\,dT_0/ds} + \Lambda_0^2\right)Q\\ = I_{c1}\delta(s - x_{c0}) - \frac{x_{c1}}{x_{c0}}\left(\frac{d}{ds} - k^2 s\right)\bar{K}T_0^{\frac{1}{2}}\frac{dT_0}{ds},\end{aligned} \tag{A.4}$$

where $Q \propto T_0^{\frac{1}{2}} \times$ (magnetic field) is a heating rate, whose equation was obtained from the linearized equations for electron momentum, Ampere and Faraday:

$$\left(\frac{d^2}{ds^2} - k^2\right)Q + \frac{d}{ds}\left\{\frac{Q}{T_0}\frac{dT_0}{ds}\left[\tfrac{3}{2} + \frac{\Lambda_0^2}{\alpha_0\gamma_0'}\left(\beta_0'' - \frac{\delta_0\gamma_0 n_0 v_0}{\bar{K}T_0^{\frac{1}{2}}\,dT_0/ds}\right)\right]\right\} + k^2\frac{v_0}{\alpha_0}\left(n_1\frac{dT_0}{ds} - T_1\frac{dn_0}{ds}\right) = 0. \tag{A.5}$$

Here $\bar{m}$ is the ion mass per unit charge; $\bar{K}$ is the coefficient in Spitzer's classical heat flux; m_e is the electron mass; α_0, β_0'', γ_0, γ_0'', δ_0 are functions of Z_I given by Braginskii (1965); and Λ_0 is $\Lambda_c(T_0/T_{c0})^2(n_c/n_0)^{\frac{1}{2}}$, where $\Lambda c \equiv (m_e\gamma_0'/\delta_0\gamma_0^2)^{\frac{1}{2}}(2\pi\bar{K}T_{c0}^2/\lambda n_c)$, representing the ratio of electron mean-free path to laser wavelength.

subito e.V. licensed customer copy supplied and printed for Universidad Politecnica de Madrid. Servicio de Coordinacion de Bibliotecas (SLI04X00177E)

REFERENCES

BRAGINSKII, S. I. 1965 *Reviews of Plasma Physics*, Vol. 1 (Consultants Bureau, New York)

DENG XIMING & YU, WENYAN 1984 *Advances in ICF*, C. YAMANAKA ed. (ILE, Osaka p. 66).

ESTABROOK, K., KRUER, W. L. & BAILEY, D. S. 1985 *Physics Fluids* **28**, 19.

GARDNER, J. H. & BODNER, S. E. 1981 *Phys. Rev. Lett.* **47**, 1137.

KATO, Y. *et al.* 1984 *Phys. Rev. Letters* **53**, 1057.

LANDAU, L. D. & LIFSHITZ, E. M. 1980 *Electrodynamics of Continuous Media*, (Pergamon, New York).

LIN ZUNQUI *et al.* 1986 *Laser and Particle Beams* **4**, 223.

OBENSCHAIN, S. P. *et al.*, 1986 *Phys. Rev. Lett.* **56**, 2807.

PEREZ-SABORID, M., BARRERO, A. & SANZ, J. (Submitted to Physics Fluids).

SANMARTIN, J. R., SANZ, J. & NICOLAS, J. A. 1987 *Phys. Lett. A* **124**, 81.

SANZ, J. *et al.* 1988 *Physics Fluids*, **31**, 2320.

VAN DYKE, M. 1964 *Perturbation Methods in Fluid Mechanics*, (Academic, New York).

subito e.V. licensed customer copy supplied and printed for Universidad Politecnica de Madrid. Servicio de Coordinacion de Bibliotecas (SLI04X00177E)